NANO LETTERS

2008
Vol. 8, No. 7
1929-1935

Individualized Silica Nanohelices and Nanotubes: Tuning Inorganic Nanostructures Using Lipidic Self-Assemblies

Thomas Delclos,[†,‡] Carole Aimé,[†] Emilie Pouget,[§] Aurélie Brizard,[†] Ivan Huc,[†] Marie-Hélène Delville,[*,‡] and Reiko Oda[*,†]

Institut Européen de Chimie et Biologie, Université de Bordeaux CNRS UMR 5248, 2 rue Robert Escarpit, 33607 Pessac, France, Laboratory of Macromolecular and Organic Chemistry, Eindhoven University of Technology, Den Dolech 2, 5612AZ Eindhoven, The Netherlands, and Institut de Chimie de la Matière Condensée de Bordeaux, Université de Bordeaux UPR CNRS 9048, 87 avenue du Dr Albert Schweitzer, 33608 Pessac, France

Received March 5, 2008; Revised Manuscript Received April 28, 2008

ABSTRACT

Diverse chiral nanometric ribbons and tubules formed by self-assembly of organic amphiphilic molecules could be transcribed to inorganic nanostructures using a novel sol−gel transcription protocol with tetraethoxysilane (TEOS) in the absence of catalyst or cosolvent. By controlling parameters such as temperature or the concentration of the different reactants, we could finely tune the morphology of the inorganic nanostructures formed from organic templates. This fine-tuning has also been achieved upon controlling the kinetics of both organic assembly formation and inorganic polycondensation. The results presented herein show that the dynamic and versatile nature of the organic gels considerably enhances the tunability of inorganic materials with rich polymorphisms.

In Nature, many examples exist of inorganic nanostructures with well-defined architectures and functions.[1] The diversity of their morphologies and their exquisite organization have inspired the scientific community to explore their potential use in the development of materials,[2,3] such as nanoscale electronic and sensing devices.[4] While Nature is far ahead in terms of elaborating structurally complex bioinorganic structures, the lack of fine-tunability of these objects calls for the development of synthetic methods enabling the controlled preparation of artificial nanosized architectures.[5–7] One such method is inspired from the structural diversity of self-assembled organic systems and exploits them as templates for inorganic nanomaterials formation.[8,9] In particular, this approach has previously been successfully used for the formation of silica materials with various architectures and/or controlled porosities.[10] In the past decade, sol−gel polycondensation of tetraethoxysilane (TEOS) onto organic templates has been widely used for silica materials production.[11] In this context, assemblies of amphiphilic organic molecules[12] or of peptides[13] have given rise to a broad diversity of nanometric organic templates. Here, we focus on chiral self-assemblies such as twisted or helical ribbons and tubules as templates for the formation of chiral silica structures.[3,14] These structures have been the subject of increasing attention[15] considering their many proven and potential applications.[16] Indeed, tubules provide a confined environment suitable for nanocontainers development and exhibit inner and outer surfaces that could be functionalized. Such materials with well-defined nanoscale cavities are under intensive investigation because of their potential utility as adsorbents, electron devices, and catalysts.[17] In view of these applications, it is therefore of prime importance to be able to control and fine-tune the morphologies of such nanometric materials; the extremely rich polymorphisms of organic self-assemblies allows, in some cases, morphological tuning of inorganic structures by varying parameters such as molecular structure, solvent, or the presence of salt or metals.[18,19]

In the following study, we use assemblies of amphiphilic molecules as templates for the growth of inorganic silica. The amphiphiles are cationic bis-quaternary ammonium gemini surfactants[20] having the formula C_2H_4-1,2-$((CH_3)_2N^+C_{16}H_{33})_2$, noted hereafter 16−2−16, with tartrate[21]

* Corresponding authors, r.oda@iecb.u-bordeaux.fr and delville@icmcb-bordeaux.cnrs.fr.
† Université de Bordeaux CNRS UMR 5248.
‡ Université de Bordeaux UPR CNRS 9048.
§ Eindhoven University of Technology.

10.1021/nl080664n CCC: $40.75
Published on Web 05/28/2008

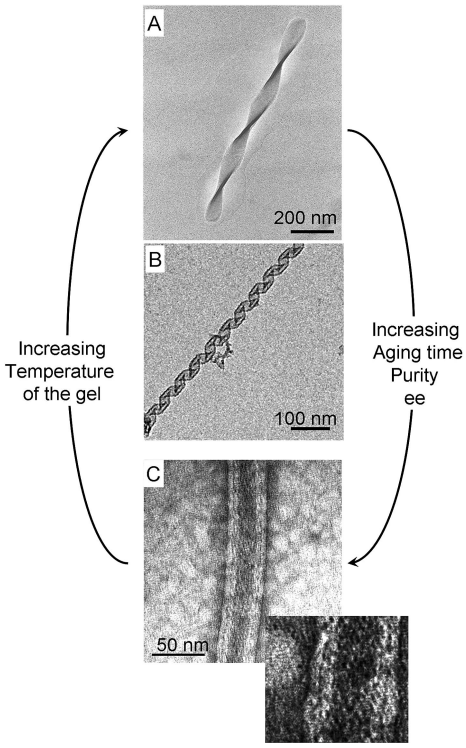

Figure 1. Transmission electron microscopy (TEM) images showing the morphological diversity of the self-assembly of gemini 16−2−16 tartrate surfactants: (A) twisted ribbon; (B) helical ribbons; (C) tubules. Upon variation of diverse independent parameters, the morphology can be finely tuned. The inset in (C) shows the double layers of the tubule wall.

as a counterion (compound **1**). Assemblies of these amphiphiles exhibit a wide diversity of morphologies that express the chirality of tartrate ions at a scale of nanometers to micrometers, including twisted and helical ribbons, as well as nanotubes. Such ribbons form a three-dimensional (3D) network and gel both water and organic solvents.[22] Of particular interest is that the morphologies of these nanometric structures can be finely tuned[23] using independent parameters such as enantiomeric excess, concentration, time, temperature, and additives (Figure 1).

Because of their structural diversity and tunability, gemini tartrates represent an ideal template for inorganic transcription. Additionally, as dicationic amphiphiles, their assemblies are expected to provide numerous sites to nucleate TEOS polymerization. In a preliminary study, the sol−gel transcription of hydrogels of these gemini tartrate was achieved by polycondensation of TEOS, with benzylamine as a catalyst in water/pyridine (1:1 vol/vol) as solvents.[18] We successfully transcribed organic twisted ribbons into silica structures with various pitches translating the enantiomeric excess of the organic template. However, in these initial experiments, substantial morphological differences were observed between the organic templates (twisted ribbons and tubules) and the final inorganic structures (double helical fibrils).

In this paper, we present the optimization of this transcription using a novel strategy that allows finely controlling the morphology of the resulting nanometric inorganic (silica) structures. This simpler and easier strategy consisted in getting rid of both the organic cosolvent and the catalyst. The sol−gel transcription of a high diversity of self-assembled 16−2−16 tartrate structures was then performed in water as a single solvent and led to silica ribbons. The structures of these inorganic ribbons could be finely tuned in various ways. Not only the parameters responsible for organic structural diversity mentioned above but also the kinetics of both organic assembly formations and the sol−gel replication process provided new ways of controlling inorganic morphologies. The major outcome of these methodological developments is the formation of isolated, individual objects, including nanotubes with homogeneous external diameters.

The preliminary results on the sol−gel transcription of twisted ribbons of 16−2−16 tartrate with variable pitches did not exactly reflect the morphologies of the organic templates as mentioned above.[18] This is most likely due to the extreme sensitivity of the self-assembly behavior of gemini tartrate templates to various parameters which has shown strong dependence on experimental procedures. In particular, a change in solvent dramatically influences the morphology of the aggregates: in the presence of an organic cosolvent such as pyridine tubule formation does not occur and sol−gel transcription only gave rise to twisted inorganic ribbons. In order to fully exploit the polymorphism of the structures of the organic assemblies, we therefore needed to develop a new procedure of transcription in the absence of pyridine.

Optimization of transcription conditions proceeded in multiple steps, considering the different relevant parameters. The experimental procedure is described in detail in the Supporting Information. In this paper, except when otherwise specified, sol−gel transcription has been carried out in pure deionized water as briefly described below. 16−2−16 tartrate was selected as a template for the generation of both inorganic nanoribbons and nanotubules. It was dispersed in water at a concentration of 5−10 mM, and the resulting mixture was heated up to 55 °C and then cooled down to room temperature leading to a gel which was aged for 3 weeks before sol−gel replication except when otherwise mentioned. At this stage, the organic gel shows the formation of a network of nanofibers. Their morphology depends on the ee of tartrate anions.[23] In the case of the pure enantiomer, e.g., 16−2−16 L (or D)-tartrate, nanotubules with an external diameter of 33.0 ± 4.5 nm and an internal diameter 20.2 ± 5.7 nm are observed. These values correspond to the wall thickness of the organic tubules of about 6.5 nm for two bilayers, as can be seen in Figure 1C.

The choice of the silica precursor, tetramethoxysilane (TMOS) vs tetraethoxysilane (TEOS), and the effect of benzylamine catalyst were tested. We have observed that when benzylamine was used along with TEOS, the polycondensation was induced too rapidly leading to the formation of additional large silica nanoparticles (Figure S1A). When TMOS, which is more reactive than TEOS, was used as precursor, only highly aggregated and ill-defined structures were observed (Figure S1B). We therefore chose to perform the following reactions without any basic catalyst and with a systematic large excess of TEOS (1000 equiv/gemini unit).

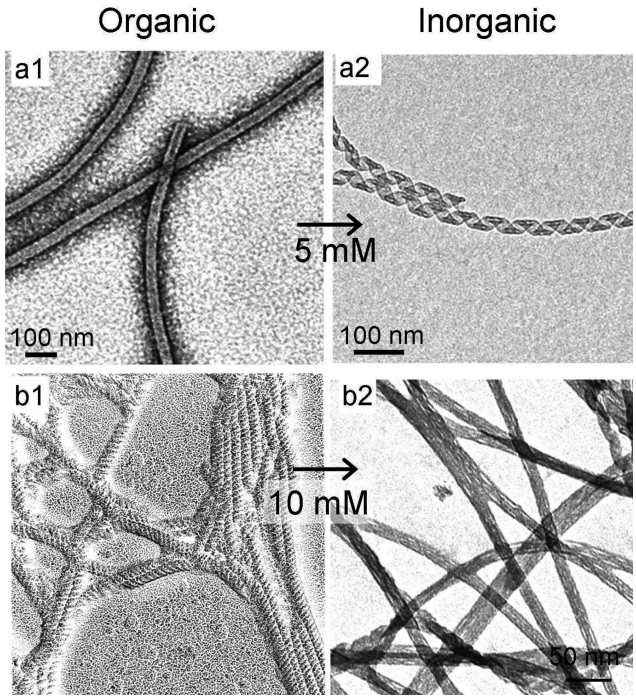

Figure 2. TEM micrographs showing the effect of the organic gel concentration on the morphology of transcribed silica structures. While 5 and 10 mM organic gels exhibited nanotubules formation with a degree of entanglement that increases with concentration (a1 and b1, respectively), morphology variations were induced upon transcription into silica replicas. Starting from a 5 mM gel, silica nanohelices were obtained (a2), while silica nanotubes were observed starting from a 10 mM gel (b2).

In a typical experiment, TEOS was prehydrolyzed in water (pH 6) for 12 h before each run[13] and then allowed to stand in contact with organic gels for 36 h at room temperature (~22 °C). In order to ensure good contact between the prehydrolyzed TEOS which remained very little miscible in water and the gel, the solution was vortexed (2000 rpm) for a few seconds at the beginning of the reaction. The rate of hydrolysis−condensation of TEOS under neutral conditions as followed by ^{29}Si NMR was very slow even in the presence of the gemini (Supporting Information, Figure S2), and the optimized silica replicates were obtained in 36 h (Supporting Information, Figure S3). The samples were then thoroughly washed with ethanol to remove all the organic components including the templates (DRIFT measurements not shown). In some cases the samples were further calcined: samples were heated under argon (temperature increase at 5 °C/min) 1 h at 100 °C, 1 h at 200 °C, and 3 h at 450 °C. Finally, the samples were heated 3 h at 450 °C under air. This thermal treatment did not modify the morphology of the inorganic objects except for a slight shrinkage (Figure S4).

Transcription of the organic templates was achieved under a number of different conditions in order to assess the role of each parameter on the final morphology of the replicated objects. Specifically, we varied the organic gel aging time, organic gel concentration, organic gel enantiomeric excess, and the temperature of both organic gel formation and silica transcription.

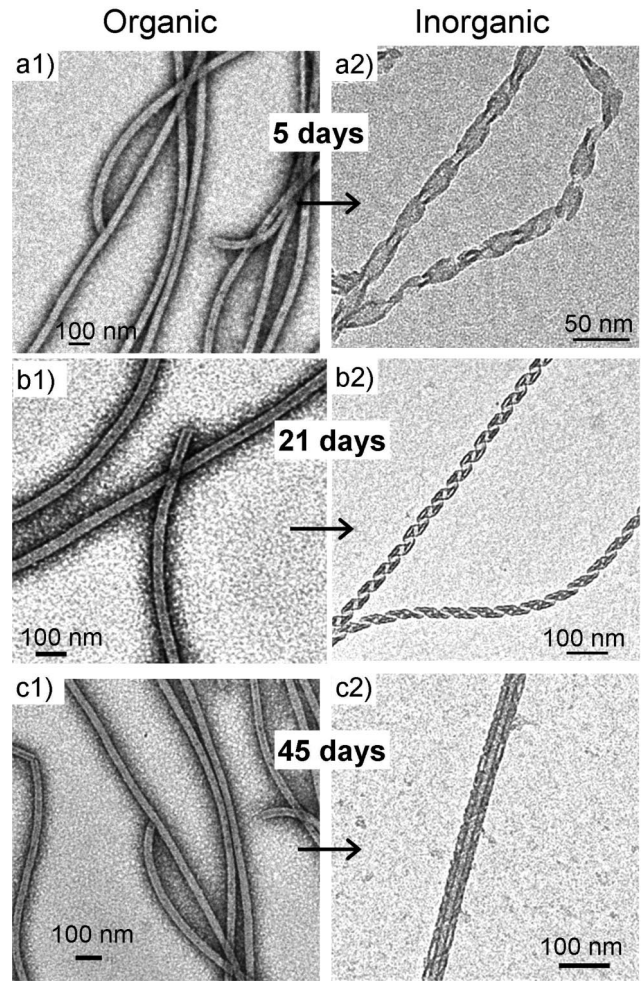

Figure 3. TEM micrographs showing the morphology of inorganic ribbons obtained upon transcribing organic 16−2−16 tartrate gels after various aging times. Organic gels show the formation of entangled networks of nanotubules of similar morphology after 5, 21, or 45 days (a1, b1, c1), respectively. Transcribing these structures at different aging times allowed controlling the morphology of inorganic chiral ribbons into twisted ribbons after 5 days (a2), helices after 21 days (b2), and nanotubes after 45 days (c2).

The concentration of the organic species is far more critical than that of the inorganic one. When it is increased from 5 to 10 mM, the organic nanotubules observed after 21 days are significantly more entangled (Figure 2, panels a1 and b1). Moreover, their transcription into inorganic structures yielded concentration-dependent morphologies. While the transcription of organic nanotubules of a 5 mM gel produced nanohelices indicating an unwinding of the organic tubules into helical ribbons (Figure 2, panels a1 → a2), the increase of the initial concentration to 10 mM resulted in silica nanotubes (Figure 2, panels b1 → b2). A possible origin of this discrepancy is the higher cohesion of the organic tubules in the 10 mM gel due to entanglement and bundle formation. Higher concentrations of organic compound did not produce well-defined inorganic structures. Therefore for the rest of the study, the concentration was fixed at 5 mM unless otherwise mentioned.

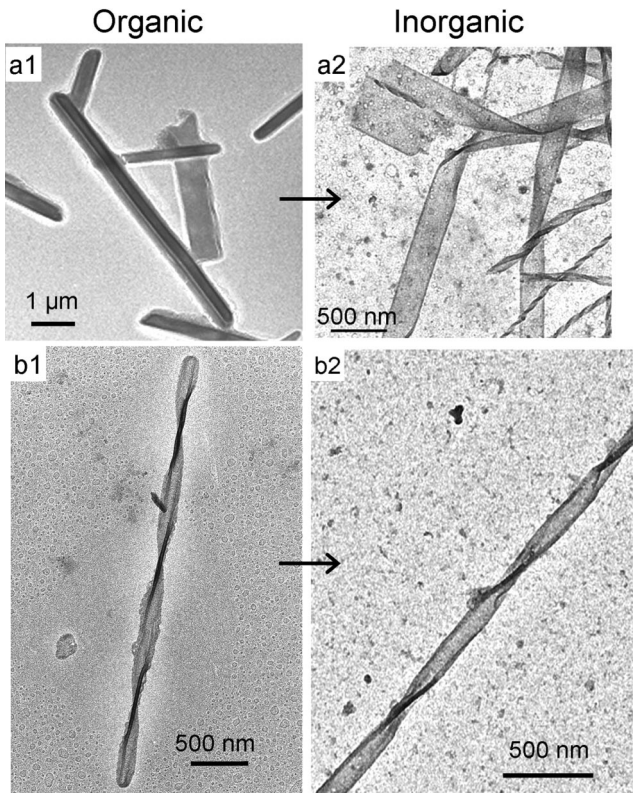

Figure 4. TEM micrographs showing the effect of adding achiral 16−2−16 Br (4.7 mol %) to 16−2−16 L tartrate gels (a1) and the effect of decreasing enantiomeric excess down to ee = 33% (b1). The transcription of these organic templates into silica structures allows preserving their morphologies and yields flat silica ribbons (a2) and twisted silica ribbons (b2), respectively.

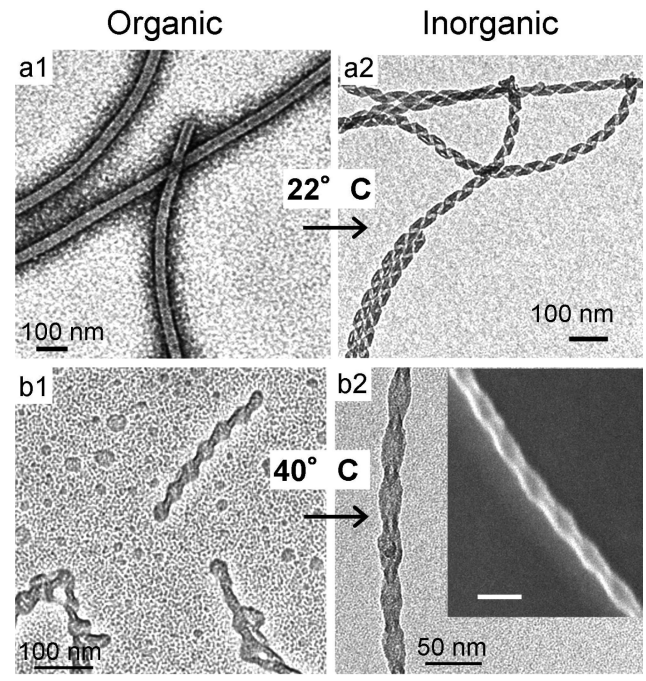

Figure 5. TEM micrographs showing the effect of temperature on organic gel morphology and the transcribed inorganic fibers that result. Organic nanotubules of 16−2−16 tartrate formed at room temperature (a1) are transcribed into helical silica (a2), while organic twisted ribbons formed at 40 °C (b1) resulted in transcription into inorganic ribbons with conserved twisted morphology (b2). The inset shows a high-resolution scanning electron microscopy (HRSEM) image of a single twisted ribbon showing the 3D nature of the object and its pitch. Bar represents 50 nm.

The formation of chiral ribbons of 16−2−16 tartrate takes place in pure water leading to the formation of helical ribbons within 3 h. Nanotubule formation then occurs after about 1.5 days.[23b] In the presence of some additives as, for example, Br^- or the opposite tartrate enantiomer, twisted ribbons are observed before helical ribbon formation (Figure 1); twisted ribbons are also a presumed intermediate for the pure 16−2−16 tartrate (ee = 1) but were not observed because of their fast conversion into helical ribbons. Furthermore, once the nanotubes are formed, no morphological transition is observed (Figure 2, panels a1, b1, c1). Nevertheless, the behavior of these nanotubes can be drastically altered during replication depending on their age. When aged for only 5 days, the nanotubules underwent an unexpected morphological change back to *twisted* ribbons during sol−gel transcription (Figure 3, panels a1 → a2)! As the organic gel was aged for a longer time, diverse inorganic structures were obtained. As mentioned above, the transcription of a 5 mM gel aged for 21 days for instance induced the formation of helical replica (Figure 3, panel b1 → b2), and it is only when the gel was aged for longer than 45 days that the transcribed structures showed the same morphology as the original organic assemblies, i.e., nanotubules (Figure 3, panels c1 → c2) exhibiting hollow cylinders as previously described with the organic template. These results suggest that the stability of the organic template increases with its age, which in turn increases its resistance to morphological changes during transcription.

Electron microscopy images do not show any morphological evolution of the organic tubular structures upon aging. This is confirmed by data obtained using other techniques such as X-ray diffraction, as well as FT-IR experiments which showed no visible evolution for the intra- and intermolecular organization of the tubules with aging times, between 1 day and several months.[23b] However, once transcribed, subtle differences in stability of organic tubules become apparent. The condensation of hydrolyzed TEOS onto the cationic gemini membrane supposes the co-complexation of both the anionic silica precursor and the tartrate counterion. The competition between the two anionic species seemed to disturb the self-assembly of gemini tartrates, unrolling tubules to helical or twisted ribbons. In this respect, the effect of the silicate ionic precursors condensing on the template during silica condensation appears to be similar to the effect of the replacement of tartrate by nonchiral anions, e.g., bromide.[23b] How the original structure is disturbed seems to be directly related to the stability of the tubules which increases with time. We did not attempt to investigate the origin of this morphological change in detail and rather focused on the advantage it provides, which is to allow the straightforward and reproducible generation of a variety of inorganic architectures from a single template, depending on experimental conditions.

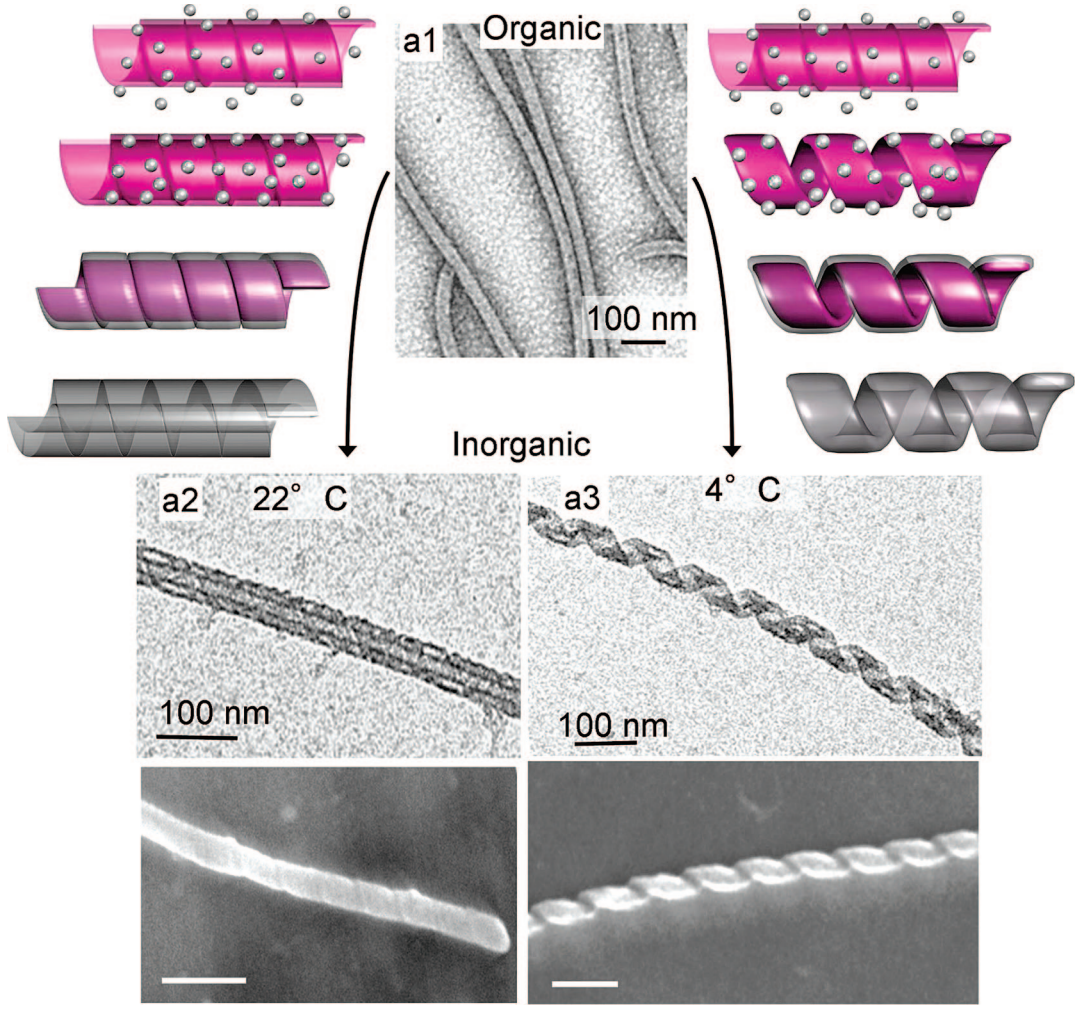

Figure 6. TEM micrographs showing the effects of the transcription temperature. Starting from gels having tubular morphology (formed at room temperature for 45 days) (a1), we observed the formation of silica nanotubules when the temperature of transcription was set at 22 °C (a2) and of silica nanohelices upon transcription at 4 °C (a3). The corresponding HRSEM images (bar represents 100 nm) of a nanotubule and a helical ribbon showing the 3D nature of the objects and its pitch for the second one.

When a high quantity (5%) of achiral molecules, 16−2−16 Br, are added to a pure sample of gemini 16−2−16 tartrate, molecular chirality is not expressed anymore in the aggregate morphology and unwound flat ribbons are observed (Figure 4, panel a1). Consistently, sol−gel transcription of these objects produced inorganic materials having similar unwound morphologies with occasional twists (Figure 4, panel a2).

In a similar way, the addition of 16−2−16 tartrate complexed with the opposite enantiomer also influences the morphology of the organic aggregate. Mixing with more than 20% of the opposite 16−2−16 tartrate enantiomers (ee = 60%) results in the formation of twisted ribbons instead of the tubular structures obtained with pure enantiomers of 16−2−16 tartrate (Figure 4, panel b1). Again, using the replication method that we have developed, we were able to transcribe the organic twisted ribbons of 16−2−16 tartrate (ee 33%) gels into silica structures while preserving their twisted morphology (Figure 4, panel b2).

The temperature of gel formation has previously been shown to be a key parameter in controlling self-assembly of 16−2−16 tartrate.[23b] The nanotubules shown in Figures 2 and 3 only form at temperatures below 35 °C, and as mentioned above, the intermediate twisted structures convert into helical ribbons and tubules so rapidly that they cannot be observed. However, upon keeping the gels at 38−40 °C, the initially formed twisted ribbons remain stable and do not evolve into helices and tubules (Figure 5, panels a1 and b1, respectively). While the templates (5 mM) aged for 21 days at room temperature were transcribed into helical structures (Figure 5, panels a1 → a2, see also Figure 3, panels b1 → b2), those aged at 40 °C yielded silica twisted ribbons (Figure 5, panels b1 → b2). In so far as the transcription is concerned, we demonstrate here that temperature of gel aging can be used to control the morphology of the inorganic silica structures.

The effect of the temperature of transcription was also investigated. In this set of experiments, the same 5 mM gels of gemini 16−2−16 L tartrate aged for 45 days at room temperature were used as starting organic structures. Under these conditions, the organic templates exhibit a tubular structure (Figure 6, panel a1, see also Figure 3, panel c1). After addition of prehydrolyzed TEOS (at 22 °C), the temperature of transcription was either kept at 22 °C or decreased to 4 °C. The inorganic silica structures after sol−gel transcription

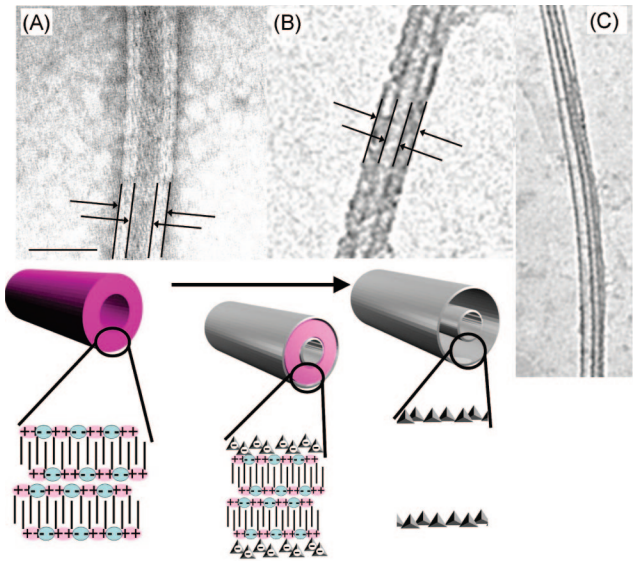

Figure 7. TEM micrographs as well as their schematic description of the structure of organic (A) and inorganic (B) nanotubules. Organic tubules exhibited two bilayers with external and internal diameters of 35.6 and 20 nm, respectively, After condensation of hydrolyzed TEOS, and washing with ethanol, the inorganic nanotubes (without calcination) exhibited an external diameter of 33 nm, with internal hollow of diameter 10 nm. The space between inner and outer shells is empty, and from time to time the inner tubes can move around and the two tubules are not coaxial (C). Bar represents 50 nm.

at 22 °C showed nanotube formation (Figure 6, panel a2, see also Figure 3, panel c1). However, when the transcription was performed at 4 °C, tubules unwound and only nanohelices were observed (Figure 6, panel a3).[24]

Why would the temperature of transcription influence the morphology of the inorganic fibers in such a way when a low temperature may be expected to stabilize organic nanotubules and prevent their unwinding? It might be pointed that lowering temperature also slows down transcription itself which may give more time for unwinding to occur before a silica shell prevents further structural changes. In short, it appears that transcription and structural changes of the template that may occur concomitantly are both kinetically controlled events and that different morphologies of final inorganic structures may be expected depending on their relative rates.

Concerning the dimensions of the silica nanotubules, statistics revealed an average external diameter of 33.0 nm which reduced to 30.7 ± 4.5 nm after calcination. This difference of 2.3 nm before and after calcination is explained by a phenomenon of shrinkage[25] occurring during calcination, inducing a decrease in diameter. If we now compare this result to the dimensions of the organic tubular template (35.6 ± 5.4 nm), we note a difference in external diameter of about 2 nm. This probably results from the required metallization of the organic tubular template to accurately measure the average external diameters.[23b] Indeed, the diameters of silica replicates observed in the same conditions, i.e., after metallization, increased up to 35.1 ± 3.9 nm. Taken altogether, these small diameter variations suggest that the layer of silicate is extremely thin, of the order of a few angstroms.

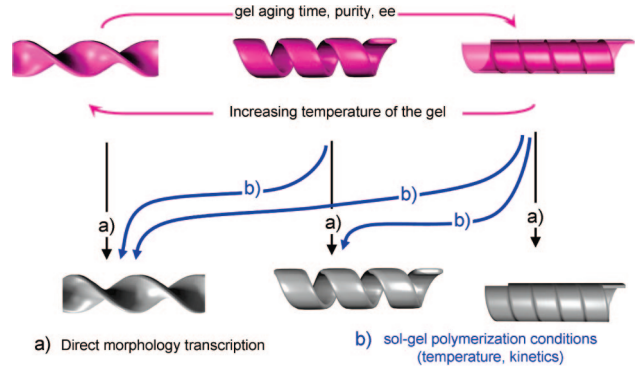

Figure 8. Schematic representation of the diversity of inorganic silica chiral ribbons. Morphological diversity of the organic template (pink arrows), inorganic structures obtained by direct replication of organic morphologies leading to identical sol−gel transcription (black arrows, a). The fine-tuning of the transcription process: aging time variation as well as replication temperature widens the potentialities of morphology controls (blue arrows, b).

TEM micrographs of the structure of organic (Figure 7A) and inorganic (Figure 7B,C) nanotubules show that the organic tubules exhibit walls with double bilayers of about 6.5 nm total thickness. The inorganic tubules show concentric tubes with internal and external silica shells which grew on both sides of the membrane surface of the organic tubules. Clearly, prehydrolyzed TEOS penetrates within the tubules and is then allowed to condense in this confined environment. When the original organic templates are removed after washings with ethanol and/or calcination, the spaces between the inner and outer shells are empty (Figures 7B and 7C).[26] Consequently, in some cases, we observed that the inner silica tubes do not remain coaxial with the outer shells as illustrated in Figure 7C. While the external diameter does not change during transcription, the diameter of the internal hollow decreases from 20 nm (Figure 7A) to about 10 nm (Figure 7B) after transcription.

The results described above rely on the extremely flexible nature of 16−2−16 tartrate gels which exhibit not only a rich polymorphism of supramolecular assemblies but also a highly versatile ability to evolve from one structure to another, allowing to finely tune not only the morphologies of the organic templates but also the structure of the inorganic replicas. This structural flexibility is further enhanced by the design of the molecule, 16−2−16 tartrate, in which chirality is introduced using ionic interaction between cationic gemini 16−2−16 and anionic tartrate; since the prehydrolyzed TEOS also interacts through ionic interaction with the ammonium functional groups of the assemblies of 16−2−16 tartrate, the competition between the two anions, tartrate vs hydrolyzed TEOS may well be the key factor for determining the morphology of the transcribed inorganic structures (Supporting Information Figure S5).

Thus, not only the polymorphism of the organic templates can be directly reflected on the morphology of inorganic silica structure but also the variation of the transcription conditions proved to be very efficient for controlling the morphologies nanosilica materials as illustrated in Figure 8.

We proposed an original way for obtaining isolated nanometric silica fibrous structures of various sizes and

shapes (ribbons, helices, and tubules). The amphiphilic system we have used as an organic template provides multiple ways to finely tune organic nanometric chiral assemblies. We took advantage of these properties to control morphologies of inorganic silica nanostructures. Competition between silica precursors and tartrate counteranions for condensation onto cationic membranes of gemini surfactants seems to influence the morphology of the silica chiral ribbons. This allowed the formation of silica twisted ribbons, precursors of helical structure formation that were not accessible with the organic templates at room temperature. Finally, simply by changing the temperature of replication, the selective formation of twisted or tubular silica has been achieved. The major advantage of the strategy developed here for the transcription as compared to what we had previously reported is that by subtle control of the parameters such as reactant concentration and kinetics of polycondensation, we are now able to drive the transcription to the desired final object morphology, from a dense network to individualized single chiral inorganic objects. This approach will certainly give access to a broad structural diversity of inorganic materials since it has proven to provide additional ways of tuning inorganic materials morphologies.

Acknowledgment. This work is supported by the CNRS, the French Ministry of Research (ACI Nanoscience), and IECB. The authors thank Dr. E. Sellier (CREMEM, Université de Bordeaux) for HRSEM assistance and Axelle Grélard (IECB, Université de Bordeaux) for NMR experiments.

Supporting Information Available: Detailed experimental conditions as well as the characterizations, additional figures describing the optimization of the sol−gel transcription process developed, and NMR data on TEOS hydrolysis in the presence or not of the organic template. This material is available free of charge via the Internet at http://pubs.acs.org.

References

(1) Davis, S. A.; Dujardin, E.; Mann, S. *Curr. Opin. Solid State Mateer. Sci.* **2003**, *7*, 273–281.
(2) Sada, K.; Takeuchi, M.; Fujita, N.; Numata, M.; Shinkai, S. *Chem. Soc. Rev.* **2007**, *36* (2), 415–435.
(3) For reviews on inorganic and hybrid materials templated from organic assemblies, see: (a) Llusar, M.; Sanchez, C. *Chem. Mater.* **2008**, *20* (3), 782–820, and references therein. (b) Sada, K.; Takeuchi, M.; Fujita, N.; Shinkai, S. *Chem. Soc. Rev.* **2007**, *36*, 415–435, and references therein.
(4) (a) Sanchez, C.; Arribart, H.; Guille-Giraud, M. M. *Nat. Mater.* **2005**, *4*, 277–288. (b) Pappas, J. L. *J. Nanosci. Nanotechnol.* **2005**, *5*, 120–130. (c) Che, S. *J. Nanosci. Nanotechnol.* **2006**, *6*, 1557–1564. (d) Wu, X.; Ruan, J.; Ohsuna, T.; Terasaki, O.; Che, S. *Chem. Mater.* **2007**, *19* (7), 1577–1583.
(5) Moreau, J. J. E.; Vellutini, L.; Man, M. W. C.; Bied, C. *J. Am. Chem. Soc.* **2001**, *123*, 1509–1510.
(6) Moreau, J. J. E.; Vellutini, L.; Man, M. W. C.; Bied, C. *Chem. Eur. J.* **2003**, *9*, 1594–1599.
(7) (a) Jung, J. H.; Shinkai, S.; Shimizu, T. *Nano Lett.* **2002**, *1*, 17–20. (b) Okamoto, K.; Shook, C. J.; Bivona, L.; Lee, S. B.; English, D. S. *Nano Lett.* **2004**, *4*, 233–239.
(8) (a) Nakamura, H.; Matsui, Y. *J. Am. Chem. Soc.* **1995**, *117*, 2651–2652. (b) Sone, E. D.; Zubarev, E. R.; Stupp, S. I. *Angew. Chem., Int. Ed.* **2002**, *41*, 1705–1709. (c) Goren, M.; Qi, Z.; Lennox, R. B. *Chem. Mater.* **2000**, *12*, 1222.
(9) (a) Shenton, W.; Pum, D.; Sleytr, U.; Mann, S. *Nature* **1997**, *389*, 585–587. (b) Davis, S. A.; Burkett, S. L.; Mendelson, N. H.; Mann, S. *Nature* **1997**, *385*, 420–423. (c) Kim, S. S.; Zhang, W.; Pinnavaia, T. J. *Science* **1998**, *282*, 1302–1305.
(10) (a) Minakuchi, H.; Nakanishi, K.; Soga, N.; Ishizuka, N.; Tanaka, N. *Anal. Chem.* **1996**, *68*, 3498–3501. (b) Sonnenburg, K.; Adelhelm, P.; Antonietti, M.; Smarsly, B.; Nöske, R.; Strauch, P. *Phys. Chem. Chem. Phys.* **2006**, *8*, 3561–3566. (c) Okamoto, K.; Shook, C. J.; Bivona, L.; Lee, S. B.; English, D. S. *Nano Lett.* **2004**, *4*, 233.
(11) (a) Ono, Y.; Nakashima, K.; Sano, M.; Kanekiyo, Y.; Inoue, K.; Hojo, J.; Shinkai, S. *Chem. Commun.* **1998**, *n/a*, 1477–1478. (b) Jung, J. H.; Ono, Y.; Shinkai, S. *Chem. Eur. J.* **2000**, *6*, 4552–4557. (c) Jung, J. H.; Kobayashi, H.; Masuda, M.; Shimizu, T.; Shinkai, S. *J. Am. Chem. Soc.* **2001**, *123*, 8785–8789.
(12) (a) Kunitake, T.; Okahata, Y.; Shimomura, M.; Yasunami, S.; Takarabe, K. *J. Am. Chem. Soc.* **1981**, *103*, 5401–5413. (b) Kunitake, T. *Angew. Chem., Int. Ed.* **2003**, *31*, 709–726.
(13) Pouget, E.; Dujardin, E.; Cavalier, A.; Moreac, A.; Valéry, C.; Marchi-Artzner, V.; Weiss, T.; Renault, A.; Paternostre, M.; Artzner, F. *Nat. Mater.* **2007**, *6* (6), 434–439.
(14) (a) Ono, Y.; Nakashima, K.; Sano, M.; Hojo, J.; Shinkai, S. *Chem. Lett.* **1999**, *n/a*, 1119–1120. (b) Jung, J. H.; Ono, Y.; Shinkai, S. *Angew. Chem., Int. Ed.* **2000**, *39*, 1862–1865. (c) Jung, J. H.; Ono, Y.; Hanabusa, K.; Shinkai, S. *J. Am. Chem. Soc.* **2000**, *122*, 5008–5009. (d) Yang, Y.; Suzuki, M.; Owa, S.; Shirai, H.; Hanabusa, K. *J. Mater. Chem.* **2006**, *16*, 1644–1650. (e) Zhang, H.-F.; Wang, C.-M.; Buck, E. C.; Wang, L.-S. *Nano Lett.* **2003**, *3*, 577–580.
(15) For a review on chiral fibrous structures, see: (a) Ihara, H.; Takafuji, M.; Sakurai, T. In *Encyclopedia of Nanoscience and Nanotechnology*; Nalwa, H. S., Ed.; American Scientific Publishers: Valencia, CA, 2004; Vol. 9, pp 473−495. (b) Brizard, A.; Oda, R.; Huc, I. *Top. Curr. Chem.* **2005**, *256*, 167–218.
(16) (a) Schnur, J. M. *Science* **1993**, *262*, 1669–1676. (b) Schnur, J. M.; Ratna, B. R.; Selinger, J. V.; Singh, A.; Jyothi, G.; Easwaran, K. R. K. *Science* **1994**, *264*, 945–947. (c) Jung, J. H.; John, G.; Yoshida, K.; Shimizu, T. *J. Am. Chem. Soc.* **2002**, *124*, 10674–10675. (d) Shimizu, T.; Masuda, M.; Minamikawa, H. *Chem. Rev.* **2005**, *105*, 1401–1443.
(17) Patzke, G. R.; Krumeich, F.; Nesper, R. *Angew. Chem., Int. Ed.* **2002**, *41*, 2446–2461.
(18) Sugiyasu, K.; Tamaru, S.; Takeuchi, M.; Berthier, D.; Huc, I.; Oda, R.; Shinkai, S. *J. Chem. Soc., Chem. Commun.* **2002**, *n/a*, 1212–1213.
(19) (a) Roy, G.; Miravet, J.-F.; Escuder, B.; Sanchez, C.; Llusar, M. *J. Mater. Chem.* **2006**, *16*, 1817. (b) Ono, Y.; Nakashima, K.; Sano, M.; Hojo, J.; Shinkai, S. *J. Mater. Chem.* **2001**, *2412*, n/a. (c) Xue, P.; Lu, R.; Li, D.; Jin, M.; Bao, C.; Zhao, Y.; Wang, Z. *Chem. Mater.* **2004**, *16*, 3702. (d) Yang, Y.; Suzuki, M.; Owa, S.; Shirai, H.; Hanabusa, K. *J. Mater. Chem.* **2006**, *16*, 1644. (e) Jung, J. H.; Ono, Y.; Shinkai, S. *Langmuir* **2000**, *16*, 1643.
(20) For reviews on gemini surfactants, see: (a) Menger, F. M.; Keiper, J. *Angew. Chem., Int. Ed.* **2000**, *39*, 1906–1920. (b) *Gemini Surfactants*; Zana, R., Xia, J., Eds.;Marcel Dekker: New York, 2004.
(21) Kunarti, Eko Sri; Moran, Grainne *Mol. Cryst. Liq. Cryst.* **2005**, *440*, 71–78.
(22) Oda, R.; Huc, I.; Candau, S. J. *Angew. Chem., Int. Ed.* **1998**, *37*, 2689–2691.
(23) (a) Oda, R.; Huc, I.; Schmutz, M.; Candau, S. J.; MacKintosh, F. C. *Nature* **1999**, *399*, 566. (b) Brizard, A.; Aime, C.; Labrot, T.; Huc, I.; Berthier, D.; Artzner, F.; Desbat, B.; Oda, R. *J. Am. Chem. Soc.* **2007**, *129*, 3754.
(24) We also performed the transcription at higher temperature, (33 and 40 °C). In such cases, only the formation of spherical silica particles was observed. Clearly precursors react together too rapidly at these temperatures without replicating the template surface (data not shown).
(25) Brinker, C. J.; Scherer, G. W. *Sol-Gel Science: The Physics and Chemistry of Sol-Gel Processing*; Academic Press: San Diego, CA, 1990.
(26) We have performed IR measurements (data not shown) which showed no detectable remaining gemini tartrate after washing with ethanol.

NL080664N